2024 European Control Conference (ECC)
June 25-28, 2024. Stockholm, Sweden

Extended Lagrangian-Informed Deep Learning and Control for Electro-mechanical Systems

Nikhil Pagar, Pegah Ghaf-Ghanbari, Atul Kelkar, and Javad Mohammadpour Velni

***Abstract*—In order to accurately model the dynamics of nonlinear electro-mechanical systems, it is imperative to consider the contributions of coupling terms and dissipation. The Lagrangian formulation alone is insufficient to fully capture the holistic behavior of the system. Coupling and dissipation mechanisms play a pivotal role in shaping the system's response. Consequently, to effectively capture the dynamics of inter-coupled electro-mechanical systems with dissipation, we propose an extended Lagrangian-informed deep neural network framework in this paper. Our approach leverages the underlying physics-based knowledge of the system, incorporating it into the neural network architecture. By employing the Euler-Lagrange equations as constraints in the training process, we ensure that the learned dynamics conform to the true behavior of the system. To validate the theoretical framework, we conduct simulation experiments on a DC motor with a cart system, which serves as a representative model of dissipative nonlinear electro-mechanical systems. The experimental results demonstrate the efficacy of our approach in accurately capturing and integrating the dynamics to solve the reference tracking model predictive control design.**

***Index Terms*—Deep neural networks, Physics-informed learning, Nonlinear model predictive control, Extended Lagrangian formulation, Electro-mechanical systems**

I. Introduction

Complex electro-mechanical systems, such as high-speed trains, aero-engines and high-quality computer numerical control machine tools, are composed of numerous mechanical and electrical components. These systems are designed with discrete elements to form complex, interconnected, and highly responsive networks for transmitting power, energy and information [1]–[3]. Traditionally, dynamic models of electro-mechanical systems have been derived using fundamental principles such as Newton's laws or Lagrange's equations [4]. Even with substantial advancements in modeling and system identification techniques, the learning of complex systems remains a formidable challenge [5]. The existing literature has tackled the challenge of learning models from data through two main approaches: system identification and supervised black-box function approximation. In system identification, the kinematic structure's knowledge is leveraged, enabling the inference of linkage physics parameters using linear regression [6]. However, it is crucial to note that the learned parameters might not always be physically plausible [7]. Moreover, they are limited to linear combinations and applicable only to kinematic trees [8]. Another method involves combining the composite rigid body algorithm [9] with system identification to infer parameters of the Euler-Lagrange ordinary differential equations, including the mass matrix. On the other hand, for function approximation, standard machine learning techniques such as support vector regression [10], recurrent neural networks [11], and feedforward neural networks [12] have been employed based on the data. However, the resultant estimated models from data-driven methods often suffer from limited generalizability and interpretation [13].

By combining the strengths of both traditional modeling and data-driven methods, we can enhance system's modeling, improve predictions, and address uncertainties or inaccuracies in the existing formulations. An increasing body of research is dedicated to incorporating physics principles into the process of learning underlying dynamics [14], [15]. LINNs in [16] introduce a physics-informed energy-based neural network framework for interconnected systems under the port-Hamiltonian (pH) formalism. However, the authors in [16] did not consider the coupling or dissipation terms in the Lagrangian. Many authors also explored several cutting-edge techniques that incorporate Hamiltonian mechanics and Lagrangian knowledge within neural networks for modeling physical systems. These include Hamiltonian neural networks (HNNs), pH neural networks, DeLaN, and others [17], [17]–[20]. However, the aforementioned modeling approaches have their limitations, especially when dealing with complex electro-mechanical systems. The inherent complexity and nonlinear nature of such systems often make it challenging to derive accurate mathematical models and identification of coupling sources.

In addition, numerous control design methodologies have been proposed for control of electro-mechanical systems, including passivity-based sliding mode control [21], adaptive backstepping control [22], fuzzy adaptive control [23], H_∞ control [24], and control by feedback linearization [25]. Most of the mentioned approaches use a physics-based model of the system and lack integrating the data-driven model with control strategies. On the other hand, papers from the proposed literature integrate the learned dynamics to control the system.

Despite the advancements achieved in the aforementioned methodologies for learning and control, these approaches continue to confront inherent constraints and limitations. Most of the approaches focus specifically on mechanical subsystems, incorporating physical knowledge from Lagrangians into the neural networks to learn equations of motion from data. Additionally, the utilization of canonical data assumes prior knowledge of the target system's mass, which can be a

[1]All authors are with Clemson University, SC, USA (e-mail: npagar@clemson.edu)

restrictive assumption in certain scenarios.

This work presents a comprehensive framework for physics-informed learning and control of electro-mechanical systems characterized by dissipation and coupling. The proposed approach combines extended Lagrangian modeling with a deep neural network-based data-driven approach to capture the complex nonlinear dynamics and inter-dependencies within the control system. The key contributions are as follows:

- By incorporating physics-informed constraints to ensure adherence of the fundamental laws and physics-based principles governing electro-mechanical systems, we introduce an extended Lagrangian-informed neural network (ExLINN) approach that embeds physics-informed constraints into the neural network training process.
- For accurate data-driven modeling, our approach enables the identification and estimation of specific system parameters, including material properties, coupling coefficients and damping coefficients, supporting system design, optimization, and control.
- To solve the reference tracking problem, we employ a nonlinear model predictive control (NMPC) approach by embedding the learned ExLINN model for prediction.
- To demonstrate applicability to electro-mechanical systems characterized by nonlinearity, dissipative behavior and coupling effects, we apply our approach to a DC motor with a cart system.

II. Background and Problem Description

This section focuses on modeling electro-mechanical systems using extended Lagrangian, which capture the mutual influence between mechanical and electrical components characterized by electro-mechanical coupling. We treat electro-mechanical systems as lumped-parameter systems defined by a finite set of mechanical and electrical variables. For a comprehensive understanding of the modeling process, we encourage readers to refer [26].

A. Extended Lagrangian Model

Let $\mathcal{T}_m$ represent the energy stored in a magnetic field and $\mathcal{V}_e$ represent the energy stored in an electric field. For N electrical and M mechanical terminals, the energy transmitted to an electric and magnetic coupling field is described as [26]

$$\frac{d}{dt}(\mathcal{T}_m) = \sum_{i=1}^{N}(\dot{q})_i\frac{d\lambda_i}{dt} - \Big(\sum_{i=1}^{M}(f_e)_i\frac{dx_i}{dt} + \sum_{i=1}^{M}(\tau_e)_i\frac{d\alpha_i}{dt}\Big), \quad (1)$$

$$\frac{d}{dt}(\mathcal{V}_e) = \sum_{i=1}^{N}(e_f)_i\frac{dq_i}{dt} - \Big(\sum_{i=1}^{M}(f_e)_i\frac{dx_i}{dt} + \sum_{i=1}^{M}(\tau_e)_i\frac{d\alpha_i}{dt}\Big), \quad (2)$$

where for electrical subsystem, $\dot{q}$ is the derivative of the electric charge q w.r.t. time, λ is the flux linkage, and e_f is the coupling voltage. Similarly, within the mechanical subsystem, there exists a damper with a damping coefficient b, along with an electric or magnetic force denoted as f_e and an externally applied force f. The angular velocity is $\dot{\alpha}$, horizontal displacement is x, and τ_e is the torque. The left-hand side of (1) and (2) represent the rate of change in the stored energy over time. Conversely, the right-hand side represents the disparity between the two components. The initial component signifies the input power at the electrical terminal, while the second component denotes the input power at the mechanical terminal.

In analyzing nonlinear electro-mechanical systems, it is essential to introduce the concept of co-energy. An advantage of the coenergy lies in its capacity to compute mechanical forces and torques arising from electrical or magnetic sources. The energy and coenergy functions for the electrical subsystems are defined as [26]

$$\begin{aligned} &\text{Energy}: && \mathcal{T}_m = \mathcal{T}_m(\lambda), && \mathcal{W}_e = \mathcal{W}_e(q), \\ &\text{Coenergy}: && \mathcal{W}_m = \mathcal{W}_m(\dot{q}), && \mathcal{V}_e = \mathcal{V}_e(v), \end{aligned} \quad (3)$$

where the magnetic energy is $\mathcal{T}_m$ which is a function of the flux λ, while the magnetic coenergy, denoted by $\mathcal{W}_m$, varies with the current $\dot{q}$. On the other hand, the electric energy $\mathcal{T}_e$ is a function of the charge q, and the electric coenergy $\mathcal{W}_e$ changes with the voltage v.

For the electrical systems, the chosen coordinates to describe the system are the charge q and its derivative $\dot{q}$, as well as the flux linkage λ_f and its derivative e_f. For a system with N electrical terminals, the relationship is given by

$$\mathcal{T}_m + \mathcal{W}_m = \sum_{i=1}^{N}(\lambda_f)_i\dot{q}_i, \quad \mathcal{V}_e + \mathcal{W}_e = \sum_{i=1}^{N}(e_f)_i q_i. \quad (4)$$

The subsequent step in the modeling process involves incorporating the electro-mechanical coupling into the system's equations. For a system with a single coupled terminal, the electro-mechanical coupling equations for systems that store magnetic energy or electrical energy are as follows [26]

$$\text{Magnetic}: \mathcal{T}_m + \mathcal{W}_m = \dot{q}\lambda, \quad (5)$$
$$\Big(\frac{d\mathcal{W}_m}{d\dot{q}} - \lambda\Big)\frac{d\dot{q}}{dt} + \Big(\frac{d\mathcal{W}_m}{dx} - f_e\Big)\frac{dx}{dt} + \Big(\frac{d\mathcal{W}_m}{d\alpha} - \tau_e\Big)\frac{d\alpha}{dt} = 0,$$

$$\text{Electric}: \mathcal{V}_e + \mathcal{W}_e = vq, \quad (6)$$
$$\Big(\frac{d\mathcal{W}_e}{dv} - q\Big)\frac{dv}{dt} + \Big(\frac{d\mathcal{W}_e}{dx} - f_e\Big)\frac{dx}{dt} + \Big(\frac{d\mathcal{W}_e}{d\alpha} - \tau_e\Big)\frac{d\alpha}{dt} = 0.$$

Since dv, dx, $d\alpha$ and $d\dot{q}$ can have any values, setting the coefficients in the equations to zero, we get [26]:

$$\frac{d\mathcal{W}_e^*}{dv} = q, \ \frac{d\mathcal{W}_e^*}{dx} = f_e, \ \frac{d\mathcal{W}_e^*}{d\alpha} = \tau_e, \quad (7)$$

$$\frac{d\mathcal{W}_m^*}{d\dot{q}} = \lambda, \ \frac{d\mathcal{W}_m^*}{dx} = f_e, \ \frac{d\mathcal{W}_m^*}{d\alpha} = \tau_e. \quad (8)$$

The coupling term can be determined using the above equations depending on the system's characteristics. To avoid notational inconsistency, we denote the energy from coupling by $\mathcal{W}^*$ (the magnetic energy obtained through coupling as $\mathcal{W}_m^*$ and the electric energy as $\mathcal{W}_e^*$), while we represent magnetic coenergy as $\mathcal{W}_m$ and the electric energy as $\mathcal{W}_e$.

Now, considering L as the Lagrangian for the mechanical system, which is the difference between kinetic energy T and potential energy V, and $\mathcal{W}$ as the Lagrangian for the

electrical system which consists of $\mathcal{W}_m$ and $\mathcal{W}_e$, the extended Lagrangian $\mathcal{L}$ for electro-mechanical systems is expressed as

$$\mathcal{L} = \mathrm{L} + \mathcal{W} = (T - V) + (\mathcal{W}_m - \mathcal{W}_e). \tag{9}$$

Incorporating the electro-mechanical coupling within the extended Lagrangian framework is essential. While identifying the coupling terminal is critical, the coupling itself may not always be obvious. It is imperative to discern the nature of the energy emanating from the coupling terminal and use the established set of equations to derive the coupling energy $\mathcal{W}^*$. The coupling from the electric origin can be obtained using (7), whereas the coupling from the magnetic source can be obtained using (8). After obtaining the coupling, it needs to be added to the respective energy. The sign of addition depends on the source of coupling. Finally, the extended Lagrangian is obtained as

$$\mathcal{L} = \mathrm{L} + \mathcal{W} = (T - V) + (\mathcal{W}_m - \mathcal{W}_e) \pm \mathcal{W}^*. \tag{10}$$

Lagrangian formalism characterizes a classical physics system defined by coordinates $x = (q, \dot{q})$, originating from an initial state x_0. We use Euler-Lagrange equations to deduce the equation of motion (EOM) as

$$\frac{d}{dt}\Big(\frac{\partial \mathcal{L}}{\partial \dot{q}_i}\Big) - \frac{\partial \mathcal{L}}{\partial \dot{q}_i} = F_i - \frac{\partial D_i}{\partial \dot{q}_i}, \tag{11a}$$

$$\ddot{q} = \Big(\frac{\partial^2 \mathcal{L}}{\partial \dot{q}^2}(q, \dot{q})\Big)^{-1}\Big(F_i - \frac{\partial D_i}{\partial \dot{q}_i} - \frac{\partial^2 \mathcal{L}}{\partial q \partial \dot{q}}(q, \dot{q})\dot{q} + \frac{\partial \mathcal{L}}{\partial q}\Big), \tag{11b}$$

where D represents a dissipative function that accounts for viscous frictions and resistances, while F encompasses external forces and voltages, which are input to the system. With a specified set of coordinates $x = (q, \dot{q})$ and input $u = F$, we have established a technique for determining $\ddot{q}$ from a Lagrangian, which can be integrated to get the system's dynamics. Let the nonlinear system dynamics be

$$\dot{x}(t) = f(x(t), u(t)) \tag{12}$$

for an initial time $t_0 \in \mathbb{T}$ and the states $x : \mathbb{T} \to \mathcal{X} \subseteq \mathbb{R}^n$, given an initial condition $x_0 \in \mathbb{R}^n$, and the system input $u : \mathbb{T} \to \mathcal{X} \subseteq \mathbb{R}^m$. Let f be a continuous and locally Lipschitz continuous function of the state.

B. Control Problem

We consider the reference tracking control problem of electro-mechanical system (12) to determine control input to ensure that states of the system closely track a predefined desired reference trajectory. The system (12) is discretized at equidistant time grid, i.e., $t_k = kT_s + t_0$ resulting in the corresponding discrete states $x_k = x(t_k)$ and $u_k = u(t_k)$ for $k \in \{0, \ldots, N\}$. This problem can be solved using a nonlinear model predictive control strategy considering the cost function $J : \mathcal{X} \times \mathcal{X} \times \mathcal{U} \to \mathbb{R}^+$ which can be expressed as

$$J(x_k^{ref}, x_k, u_k) = \left\| x_k^{ref} - x_k \right\|_Q^2 + \| u_k \|_R^2 . \tag{13}$$

The matrices Q and R are the penalties on the state variables and control inputs, respectively. For each time step $k = t$, the discrete-time moving horizon optimal control problem with the horizon length of N_p for the current time instant t is

$$\min_{u_t, \ldots u_{t+N_p-1}} \mathcal{J}(x_{t+N_p}) + \sum_{k=t}^{k=t+N_p-1} J(x_k^{ref}, x_k, u_k) \tag{14a}$$

$$s.t.\ x_{k+1} = f(x_k, u_k), u_k \in \mathcal{U}, x_k \in \mathcal{X} \tag{14b}$$

where $\mathcal{J}(x_{t+N_p})$ represents the cost associated with the terminal state, and x_k^{ref} signifies the reference trajectory. The subscript k is employed to indicate a sample taken at a fixed time interval of T_s ahead of the current time t, while $k+1$ denotes the subsequent evolution. The set of input constraints is denoted by $\mathcal{U}$, and $\mathcal{X}$ represents the state constraints. Solving optimization problem (14) yields an optimal control sequence, denoted as $\mathbf{u}^* = \{u_t^*, \ldots, u_{t+N_p-1}^*\}$, for the present time step. The initial control input from this sequence is then applied, and the entire process is iteratively repeated.

In this paper, we consider the problem of learning Lagrangian dynamics for the nonlinear electro-mechanical system required in (14). Given a dataset of trajectories of the coordinates along with the input to the system, we wish to infer the learned system dynamics which can be solved to determine the next states x_{k+1}.

Problem Statement: Given the dataset of the system coordinates and input, $\{(q_i, \dot{q}_i, F_i) \to (\ddot{q}_i)\}_{i=0}^N$ for the electro-mechanical system using extended Lagrangian model, we aim to find an unknown mapping Ψ which minimizes

$$\sum_{i=0}^{N} \mathbb{D}((\ddot{q}_i), \Psi(q_i, \dot{q}_i, F_i)), \tag{15}$$

where $\mathbb{D}$ is a distance metric.

III. Proposed Methodology

In this section, we introduce Extended Lagrangian Informed Neural Networks (ExLINN) framework for physics-informed learning and control of electro-mechanical systems characterized by dissipative coupling.

A. Extended Lagrangian Informed Neural Networks (ExLINN)

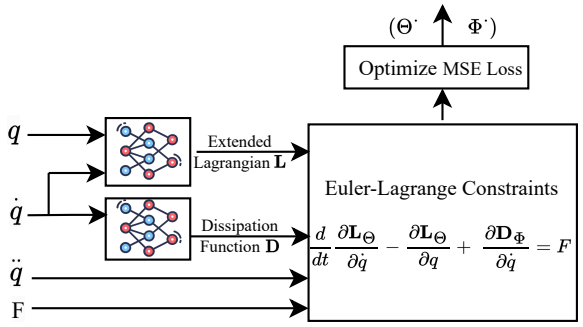

Fig. 1: Extended Lagrangian informed learning architecture

ExLINN incorporates the Lagrangian mechanics and embeds this prior knowledge into the deep learning framework. Unlike many model learning techniques, ExLINN framework employs a pair of deep neural networks (DNNs) to learn

the extended Lagrangian and dissipation function in (12). We employ DNNs to capture the inherent nonlinearity in the system dynamics, and they offer a more trainable structure due to their lower computational resource demands. We employ two distinct DNNs due to the distinct physical properties of the Lagrangian and dissipation function, which can be effectively incorporated into each respective neural network during the learning process. This will avoid the conflict in learning the functions and enhance the accuracy of the neural networks. Fig. 1 demonstrates the overview of computational process involved in learning the ExLINN. The generalized coordinates' data is utilized to learn the extended Lagrangian and dissipation function. The Euler-Lagrange equation, which represents the equation of motion (EOM), is employed as the loss function. We exploit the inherent property that the equation of motion remains true for each state variable at every data point. To assess the network's performance, predicted values are compared to the ground truth of input at the end of each iteration, yielding the loss. Minimizing this loss function optimizes the network parameters and provides an accurate Lagrangian and dissipation function.

We begin by illustrating how to form the feature functions to learn the exact Lagrangian of the underlying electro-mechanical system. The formalism uses the system's energy; therefore, the extended Lagrangian $\mathcal{L}$ is a function of the generalized coordinates $x = (q, \dot{q})$. Throughout the paper, we assume that a finite dataset $\mathcal{D}$ of system trajectories, i.e., time series data of the state variables and the input for the system, is available. Let the dataset be $\mathcal{D} = \{(x, \dot{x}), F\}$, and $x \in \{x_m, x_e\}$ where x_m represents the state variables of the mechanical subsystem, and x_e represents the state variables of the electrical subsystem. Assuming that the Lagrangian of the electro-mechanical systems is of the form (10), often, the kinetic energy is the function of the generalized velocity and potential energy is often the function of the generalized position. Also, the magnetic coenergy and electrical energy are the function of the current and charge through the circuit. Hence, the basis functions to represent the respective quantities are $\mathcal{T} = t(\dot{x}_m)$, $\mathcal{W}_m = w_m(\dot{x}_e)$, $\mathcal{V} = v(x_m)$, and $\mathcal{W}_e = w_e(x_e)$.

The coupling $\mathcal{W}^*$ in (10) can be a function of $x_m, x_e, \dot{x}_m, \dot{x}_e$ and expressed as $\mathcal{W}^* = c(x_m, x_e, \dot{x}_m, \dot{x}_e) \in (\{x_m, \dot{x}_m\} \times \{x_e, \dot{x}_e\})$ where $\times$ represents Cartesian product of two sets. Moreover, intricate dependencies on velocity and surface properties are typically associated with dissipative systems, which are effectively addressed by explicitly incorporating the dissipative drag force into the Euler-Lagrange equations. If the dissipative force varies linearly with velocity, it can be represented as a scalar potential functional of the generalized coordinates known as the Rayleigh dissipation function. The Rayleigh dissipation function, encompassing linear velocity-dependent dissipative forces in Lagrangian and Hamiltonian mechanics, is denoted as $D = r(\dot{x}_m, \dot{x}_e)$.

B. Network Optimization and Testing

We learn the dynamics Ψ (15) instead of a solution map from the dataset $\mathcal{D}$ while leveraging the prior knowledge because parameterizing dynamical equations model better approximate time-series data compared to directly estimating the next state, and physical principles are usually best expressed in the EOM. The dynamic model can be learned through two approaches: forward and reverse. Depending on the control approach, the control law is dependent either on the forward model Ψ which maps the control input to the change of the system rate, or on the inverse model Ψ^{-1} which maps the system change to the control input, i.e.,

$$\begin{aligned} \ddot{q} &= \Psi(q, \dot{q}, F), \qquad (16)\\ &= \Big(\frac{\partial^2 \mathcal{L}}{\partial \dot{q}^2}(q, \dot{q})\Big)^{-1}\Big(F_i - \frac{\partial D_i}{\partial \dot{q}_i}(\dot{q}) - \frac{\partial^2 \mathcal{L}}{\partial q \partial \dot{q}}(q, \dot{q})\dot{q} + \frac{\partial \mathcal{L}}{\partial q}\Big),\\ F &= \Psi^{-1}(q, \dot{q}, \ddot{q}), \qquad (17)\\ &= \frac{\partial^2 \mathcal{L}}{\partial \dot{q}^2}(q, \dot{q})\ddot{q} + \frac{\partial^2 \mathcal{L}}{\partial q \partial \dot{q}}(q, \dot{q})\dot{q} - \frac{\partial \mathcal{L}}{\partial q} + \frac{\partial D_i}{\partial \dot{q}_i}(\dot{q}). \end{aligned}$$

We train the ExLINN by learning an inverse model via a supervised learning task with Lagrangian DNN $\mathbf{L}(q, \dot{q}; \Theta)$ and dissipation DNN $\mathbf{D}(\dot{q}; \Phi)$ where the Θ and Φ are the network parameters. Using (11), the EL constraints are enforced to learn the optimal DNN weights while the loss function is formulated as follows to minimize the error in the inverse model (17)

$$(\Theta^*, \Phi^*) = \arg\min_{\Theta, \Phi} l(\Psi^{-1}(\Theta, \Phi), F) + \lambda \Omega(\Theta, \Phi),$$

where, Ω denotes the L_2 regularization term within the loss function, while λ is weight associated with it. While testing the ExLINN, we use the forward model (16) to predict the $\ddot{q}$ using the optimized parameters (Θ^*, Φ^*).

C. Control Strategy with ExLINN

Given the learned $\mathbf{L}(q, \dot{q}; \Theta^*)$ and $\mathbf{D}(\dot{q}; \Phi^*)$ using (16) by the ExLINN approach, we can formulate a nonlinear model predictive control (NMPC) problem (14) to design the control policy for the electro-mechanical system (12). We learned the underlying model (16) instead of the solution map that takes from any initial state to the next step. At each time step, we use the learned $\mathbf{L}$ and $\mathbf{D}$ to solve the forward model (16) which is used as the prediction model in NMPC framework. The receding horizon optimal control problem described

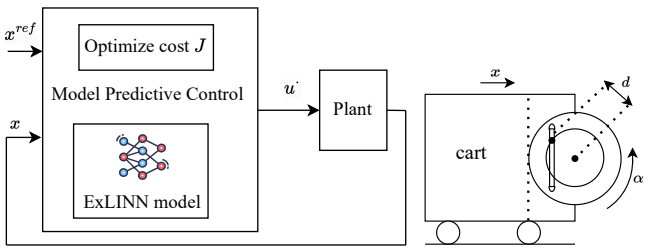

Fig. 2: Model Predictive Control with ExLINN-based qLPV model (left), DC motor with cart system (right)

in 14 requires solving the underlying system dynamics; we implement the fourth-order Runge-Kutta method, a widely accepted approach for fixed-time step integration, although

utilizing alternative solver schemes remains a possibility. Fig. 2 (left) and Algorithm 1 present the detailed steps involved in NMPC design.

Algorithm 1: Model predictive control with ExLINN

1 Execute the following commands at each time step $t_i \in \mathrm{N}$ during sampling interval $[t_i, t_i + h]$;
2 Measure states $q, \dot{q}$ from plant;
3 Estimate system model parameters by inference from the learned ExLINN;
4 Formulate optimization problem (14);
5 Solve (14) to get optimal input sequence $\mathbf{u}^*$ for the prediction horizon N_p;
6 Apply the first element from $\mathbf{u}^*$.

IV. Case Study: DC Motor with Cart

Simulation results are shown to demonstrate the performance of the proposed method using a DC motor connected to a cart via a scotch-yoke structure, as shown in Fig. 2 (right). Here, v, Q and $\dot{Q}$, α, L, and r represent the voltage source, electric charge and current, angular displacement of the disk, electric inductance, and resistance, respectively. d represents the distance associated with the pin's eccentricity. The scotch-yoke mechanism converts rotational motion from the disk into the translational motion of the cart.

The electrical subsystem is characterized by current $I_L = \dot{Q}$ and the mechanical subsystem by angular displacement and velocity $\alpha, \dot{\alpha}$. Hence, the extended Lagrangian is modeled using generalised coordinates $(\alpha, \dot{\alpha}, \dot{Q})$. In the case of electro-mechanical coupling, which involves the storage of magnetic energy in the coupling terminal, from the six equations presented in [26], $\frac{d\mathcal{W}_m^*}{d\alpha} = \tau_e$ is applicable. The torque τ_e is directly proportional to the armature current $\dot{Q}$ in most DC motors, and the magnetic field strength is represented by the motor electromagnetic force constant, k_e. Substituting $\tau_e = k_e\dot{q}$, we get, $\frac{d\mathcal{W}_m^*}{d\alpha} = k_e\dot{Q} \implies \mathcal{W}_m^* = k_e\dot{Q}\alpha$. Due to the scotch-yoke structure, the cart's horizontal displacement x can be represented as a function of angular displacement α, i.e., $x = d\cos\alpha \implies \dot{x} = -d\sin\alpha\ \dot{\alpha}$. Substituting in the kinetic coenergy we get $T = \frac{j_m\dot{\alpha}^2}{2} + \frac{m_c\dot{x}^2}{2} = \frac{j_m\dot{\alpha}^2}{2} + \frac{m_c(-d\sin\alpha\dot{\alpha})^2}{2}$. The potential and electrical energy for this system are zero, i.e., $\mathcal{W}_e = 0$ and $V = 0$. The magnetic coenergy is given as $\mathcal{W}_m + \mathcal{W}_m^* = \frac{l\dot{Q}^2}{2} + k_e\dot{Q}\alpha$. Now, the extended Lagrangian for the dc motor and cart system is formed as follows:

$$\mathcal{L} = \frac{j_m\dot{\alpha}^2}{2} + \frac{m_c(-dsin(\alpha)\dot{\alpha})^2}{2} + \frac{l\dot{Q}^2}{2} + k_e\dot{Q}\alpha. \tag{18}$$

The generalized force for the mechanical coordinate α is given by $F_1 - \frac{\partial D_1}{\partial\dot{\alpha}}$. $F_1 = 0$ and $D_1 = \frac{b_m\dot{\alpha}^2}{2}$ is the dissipation energy in the mechanical subpart due to the viscous damping. Similarly, for the electrical subsystem, the generalized forces are $F_2 - \frac{\partial D_2}{\partial\dot{Q}}$. $F_2 = v$ and $D_2 = \frac{r\dot{Q}^2}{2}$ is the dissipation energy due to the resistive effects. Now, the EOM using the EL condition for the respective coordinates is given by (11). The dynamical equations are given by [26]:

$$\ddot{\alpha}[j_m + m_cd^2\sin^2\alpha] + \dot{\alpha}[b_m + m_cd^2\sin\alpha\cos\alpha\dot{\alpha}] - k_e\dot{Q} = 0,$$
$$l\ddot{Q} + r\dot{Q} + k_e\dot{\alpha} = v. \tag{19}$$

A. Learning Results

We generated training data trajectories by fixing the DCwC coefficients to the values $j_m = 0.1, b_m = 0.5, k_e = 1, l = 1, r = 5$, and simulating until $t_f = 10$ seconds with a time step of $\Delta t = 1e^{-3}$. We used $v = 2(0.5\sin(2t) + 2)$ as the input voltage, where t is simulation time. The data is divided into training and testing sets with an 80-20 split ratio. In our approach, both DNNs are implemented as a multilayer perceptron (MLP) with Rectified Linear Unit (ReLU) activation functions and a single hidden layer containing 4 neurons. The training of both DNNs is performed simultaneously using the mean squared error (MSE) loss function. The training process is executed over 20 epochs, utilizing the Adam optimizer with a learning rate of $1e^{-3}$ and a weight decay of $1e^{-5}$. Using a multi-sine signal for testing, we explore a wide range of frequencies and interactions, validating the network's ability to capture complex data relationships. This comprehensive examination across diverse frequency domains verifies the model's robustness and predictive applicability to various input conditions.

Fig. 3 compares the measured ground truth to the ExLINN model by presenting current and angular velocity over a span of 2000 data points (equivalent to 2 seconds). We compute the average MSE for testing, which is $1e^{-2}$, and upon comparing the predicted states with the ground truth data, it becomes evident that ExLINN effectively captures the dynamics of the DCwC system. The results of estimated model with a test voltage signal using forward dynamics, i.e., angular velocity $\ddot{\alpha}$, inductor current $\dot{I}_L$, Lagrangian and the dissipation function are depicted in Fig. 3.

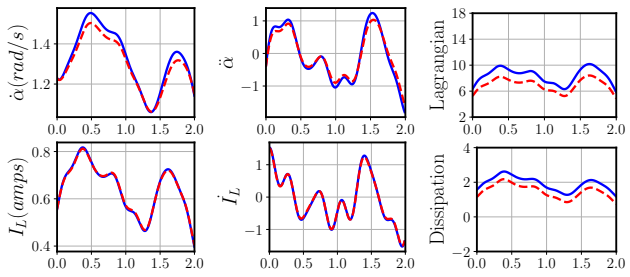

Fig. 3: Responses of the learned dynamical model (–) on the test data set (- - ground truth) w.r.t time in seconds

B. Nonlinear Model Predictive Control Results

The learned dynamical model is now combined with the model predictive control as described in Section III-C to solve the tracking control problem of the cart. The cart's movement x in the horizontal direction is restricted due to the scotch yoke mechanism in the system. Since the x is the function of the angular displacement α, we converted the desired trajectory

x^* in terms of the α and then substituted the corresponding α^* into the cost function of NMPC. For this reference tracking problem, we set the penalty coefficients as $Q = 10$ and $R = 1e^{-3}$ and opted for a prediction horizon of $N_p = 30$. Fig. 4 plots the cost of the optimization problem J, input voltage v, the cart position x and the corresponding angular displacement α, showing that the position of the cart successfully tracks the desired trajectory using the dynamical model learned by ExLINN approach.

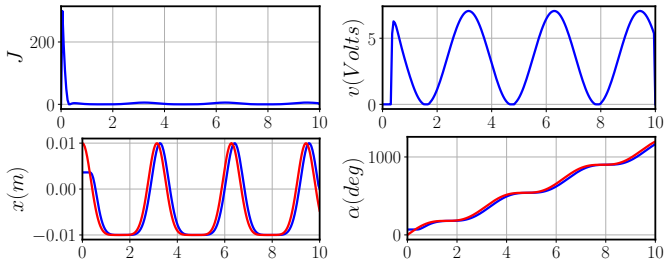

Fig. 4: NMPC optimization cost J, input voltage v, cart horizontal movement trajectory x, and angular velocity α with – predicted and – ground truth trajectories.

V. Conclusion

This work presents a comprehensive framework ExLINN for the modeling of coupled, nonlinear dissipative electro-mechanical systems. The ExLINN model exhibited strong learning capability, accurately capturing the complex dynamics of the DC motor-cart system. Through training and testing, we verified ExLINN's predictive performance to unseen complex voltage input waveforms, showcasing its capability to handle diverse frequency domains and complex system behaviors. The integration of ExLINN in NMPC further demonstrates its practical utility for control design. The NMPC approach successfully tracked a desired cart trajectory, highlighting the successful integration of our learned dynamics model into MPC. In a future work, we will extend our approach to encompass comprehensive robustness and stability analysis, with the ultimate goal of applying it to real-world systems, particularly in the context of online implementation of NMPC.

References

[1] I. Eker, "Experimental on-line identification of an electromechanical system," *ISA transactions*, vol. 43, no. 1, pp. 13–22, 2004.

[2] M. Yu, C. Xiao, W. Jiang, S. Yang, and H. Wang, "Fault diagnosis for electromechanical system via extended analytical redundancy relations," *IEEE Transactions on Industrial Informatics*, vol. 14, no. 12, pp. 5233–5244, 2018.

[3] Y. Liang, Z. Gao, J. Gao, R. Wang, Q. Liu, and Y. Cheng, "A new method for multivariable nonlinear coupling relations analysis in complex electromechanical system," *Applied Soft Computing*, vol. 94, p. 106457, 2020.

[4] A. Janot, P. C. Young, and M. Gautier, "Identification and control of electro-mechanical systems using state-dependent parameter estimation," *International Journal of Control*, vol. 90, no. 4, pp. 643–660, 2017.

[5] J. Schoukens and L. Ljung, "Nonlinear system identification: A user-oriented road map," *IEEE Control Systems Magazine*, vol. 39, no. 6, pp. 28–99, 2019.

[6] C. G. Atkeson, C. H. An, and J. M. Hollerbach, "Estimation of inertial parameters of manipulator loads and links," *The International Journal of Robotics Research*, vol. 5, no. 3, pp. 101–119, 1986.

[7] J.-A. Ting, M. Mistry, J. Peters, S. Schaal, and J. Nakanishi, "A bayesian approach to nonlinear parameter identification for rigid body dynamics," 08 2006.

[8] M. V. M. W. Spong, S. Hutchinson, *Robot modeling and control*. New York: Wiley, 2006.

[9] M. W. Walker and D. E. Orin, "Efficient Dynamic Computer Simulation of Robotic Mechanisms," *Journal of Dynamic Systems, Measurement, and Control*, vol. 104, no. 3, pp. 205–211, 09 1982.

[10] Y. Choi, S.-Y. Cheong, and N. Schweighofer, "Local online support vector regression for learning control," in *2007 International Symposium on Computational Intelligence in Robotics and Automation*. IEEE, 2007, pp. 13–18.

[11] E. Rueckert, M. Nakatenus, S. Tosatto, and J. Peters, "Learning inverse dynamics models in o (n) time with lstm networks," in *2017 IEEE-RAS 17th International Conference on Humanoid Robotics (Humanoids)*. IEEE, 2017, pp. 811–816.

[12] F. D. Ledezma and S. Haddadin, "First-order-principles-based constructive network topologies: An application to robot inverse dynamics," in *2017 IEEE-RAS 17th international conference on humanoid robotics (Humanoids)*. IEEE, 2017, pp. 438–445.

[13] M. Lutter, J. Silberbauer, J. Watson, and J. Peters, "A differentiable newton-euler algorithm for real-world robotics," 2021.

[14] Y. D. Zhong and N. Leonard, "Unsupervised learning of lagrangian dynamics from images for prediction and control," in *Advances in Neural Information Processing Systems*, H. Larochelle, M. Ranzato, R. Hadsell, M. Balcan, and H. Lin, Eds., vol. 33. Curran Associates, Inc., 2020, pp. 10 741–10 752.

[15] C. Allen-Blanchette, S. Veer, A. Majumdar, and N. E. Leonard, "Lagnetvip: A lagrangian neural network for video prediction," 2020.

[16] Y. Bao, V. Thesma, A. Kelkar, and J. M. Velni, "Physics-guided and energy-based learning of interconnected systems: from lagrangian to port-hamiltonian systems," in *2022 IEEE 61st Conference on Decision and Control (CDC)*, 2022, pp. 2815–2820.

[17] Z. Chen, J. Zhang, M. Arjovsky, and L. Bottou, "Symplectic recurrent neural networks," *arXiv preprint arXiv:1909.13334*, 2019.

[18] S. Greydanus, M. Dzamba, and J. Yosinski, "Hamiltonian neural networks," in *Advances in Neural Information Processing Systems*, H. Wallach, H. Larochelle, A. Beygelzimer, F. d'Alché-Buc, E. Fox, and R. Garnett, Eds., vol. 32. Curran Associates, Inc., 2019.

[19] G. Verdon, M. Broughton, J. R. McClean, K. J. Sung, R. Babbush, Z. Jiang, H. Neven, and M. Mohseni, "Learning to learn with quantum neural networks via classical neural networks," 2019.

[20] W. Sienko, W. Citko, and D. Jakóbczak, "Learning and system modeling via hamiltonian neural networks," in *Artificial Intelligence and Soft Computing - ICAISC 2004*, L. Rutkowski, J. H. Siekmann, R. Tadeusiewicz, and L. A. Zadeh, Eds. Berlin, Heidelberg: Springer Berlin Heidelberg, 2004, pp. 266–271.

[21] K. Fujimoto, T. Baba, N. Sakata, and I. Maruta, "A passivity-based sliding mode controller for a class of electro-mechanical systems," *IEEE Control Systems Letters*, vol. 6, pp. 1208–1213, 2022.

[22] R. Coban, "Adaptive backstepping control design for electromechanical systems," in *2017 IEEE First Ukraine Conference on Electrical and Computer Engineering (UKRCON)*, 2017, pp. 267–270.

[23] A. I. Reshetilo, P. V. Sokolov, and E. N. Karuna, "Fuzzy adaptive controller for electromechanical system," in *2019 III International Conference on Control in Technical Systems (CTS)*, 2019, pp. 101–103.

[24] Y. Hafeez and S. S. A. Ali, "Discrete-time h_∞ control of a class of underactuated electromechanical systems," in *2016 6th International Conference on Intelligent and Advanced Systems (ICIAS)*, 2016, pp. 1–5.

[25] A. Lozynskyy, Y. Marushchak, O. Lozynskyy, and L. Kasha, "Synthesis of combine feedback control of electromechanical system by feedback linearization method," in *2020 IEEE Problems of Automated Electrodrive. Theory and Practice (PAEP)*, 2020, pp. 1–6.

[26] W. Manhães, R. Sampaio, R. Lima, P. Hagedorn, and J.-F. Deü, "Lagrangians for electromechanical systems," *Mecánica Computacional*, vol. 36, no. 42, pp. 1911–1934, 2018.